Pakistan J. Zool., pp 1-12, 2025. **DOI**: https://dx.doi.org/10.17582/journal.pjz/20230907062500

Improving Resistance to *Listeria monocytogenes* by the Richness and Diversity of the Host Gut Biome through Administration of the Gallic Acid Irradiated by Ultraviolet

Min Lv[1], Wei Ge[1], Lifang Yang[2], Xu Luo[1], Chuanyan Pan[1], Shiya Ya[1], Qiufeng Ruan[1], Weijie Chen[1], Shutian Ma[1]* and Huawei Ma[1]*

[1]*Aquatic Food Processing and Preservation, Guangxi Academy of Fishery Sciences, Nanning 530021, Guangxi, China.*
[2]*College of Chemistry and Chemical Engineering, Guangxi Minzu University, Nanning 530066, China.*

Min Lv and Wei Ge are equal first authors.

Article Information
Received 07 September 2023
Revised 25 November 2024
Accepted 16 December 2024
Available online 03 March 2025 (early access)

Authors' Contribution
HM, SM: Funding acquisition, conceptualization, methodology, formal analysis, investigation, writing-original draft. ML and WG: Conceptualization, methodology, formal analysis, writing-original draft, validation, investigation. XL and CP: Writing-original draft, investigation. SY and WC: Investigation, data curation, writing-review and editing. LY and QR: data curation, writing-review.

Key words
Gallic acid (GA), UV-C, Microorganisms, Gut microbiome, *Listeria monocytogenes*

ABSTRACT

This study examined the response of specific gut bacterial species to infection with *Listeria monocytogenes* and the effect of UVC-GA on the gut microbiome over a 25-day period. Healthy mice were used as a control cohort (CC). We compared the gut microbiota profiles of the treated cohort (TC) and negative cohort (NC) to analyze the impact of UVC-GA on microbial richness and diversity. Both the gut bacterial profiles were altered following infection or treatment with *L. monocytogenes*. The *Lactobacillus* and *Photobacterium* genera were found to be decreased in all NCs, but the numbers were higher in the TCs. On the other hand, the *Bifidobacterium* and *Bacteroides* genera in all TCs were higher than those in the NCs. The infected individuals who received oral UVC-GA showed significantly increased species richness and diversity of gut microbiota, as well as a higher survival ratio of protective devices (PDs). This study provides valuable insights into the potential of UVC-GA as a probiotic in preventing Listeriosis infection by enhancing the diversity and richness of the gut microbiome.

INTRODUCTION

The gut microbiota plays a crucial role in nutrient breakdown and disease resistance, thereby contributing to the overall health of the host (Xiong *et al*., 2017). Infections of the intestinal flora by pathogenic bacteria can disrupt the balance of the microbiota, leading to health problems. Specifically, the presence of *Listeria monocytogenes* can significantly impact the microbial communities in the host gut, resulting in detrimental effects on overall health (Bernbom *et al*., 2006). *L. monocytogenes* is a gram-positive, rod-shaped bacterium that typically forms single short chains, and possesses the ability to withstand drying and freezing conditions (Theivagt *et al*., 2006). Due to its ability to grow at low temperatures, *L. monocytogenes* is considered one of the primary pathogens that pose a threat to human health, particularly in refrigerated food (Harvey *et al*., 2007). Listeriosis is a severe infection caused by consuming food contaminated with *L. monocytogenes*, with a mortality rate exceeding 25% (Sallami *et al*., 2006). People with a weak immune system like older, pregnant ladies, and newborns are most susceptible (Lagier *et al*., 1996). Recently, *L. monocytogenes* has also been isolated from the intestinal tract of small percentage of the apparently healthy human population (Guo *et al*., 2016). Emerging evidence over recent decades has stressed the importance of gut microbial diversity and richness and genes functioning in diseases. It is the fundamental element in the maintenance of the host's health and immune system. The diversity and richness of the gut microbiome can increase the resistance against pathogenic microbes, and immunity of the host, thus, improving host survival chances (Lawley *et al*.,

* Corresponding author: ma463543285@126.com, n15296527261@163.com
0030-9923/2025/0001-0001 $ 9.00/0

2013). Host health management during *L. monocytogenes* infection has received attention towards its therapy through the diversity and richness of the gut microbiome (Tran *et al*., 2013). Therefore, the study of the intestinal flora model for different pathogenic bacteria infections has become the focus of food and drug research.

Photodynamic germicidal technology is a new non-thermal germicidal method, which is used in disease treatment, food preservation, antibacterial material, and other fields (Ren *et al*., 2020). At present, photodynamic therapy can play a synergistic role with polyphenols or quinones to improve intestinal antibacterial ability and maintain the diversity and richness of intestinal microbiota (Sanhueza *et al*., 2017; Wang *et al*., 2017). This may be a new approach to preventing Listeriosis by improving the diversity and richness of the gut microbiome. Gallic acid is a kind of phenolic compound from plants, which has broad-spectrum antibacterial and antioxidant effects, several reports have declared that gallic acid (GA) in coordination with UV light can inhibit a variety of planktonic bacteria, biofilms, and fungi via producing reactive oxygen species (ROS) and decomposing bacterial membranes (Nohynek *et al*., 2006; Nakamura *et al*., 2015). Nakamura *et al*. (2015) and Wang *et al*. (2017) reported that GA solutions irradiated by UV rays can exhibit enhanced antibacterial properties. The number of *L. monocytogenes* and *Escherichia coli* on the treated surface of spinach was significantly higher in GA solutions without any radiation than that of GA solution irradiated by UV for 24 h (Ding *et al*., 2018; Gupta *et al*., 2007). In addition, applications of GA can improve gut bacterial richness and its diversity, which stimulates the host immune system, and ultimately increases the host's tolerance (Inada *et al*., 2020). Rolhion *et al*. (2019) reported that *L. monocytogenes* could destroy the diversity and richness of host gut microbiota, resulting in the imbalance of gut bacteria, thus causing listeriosis. The beneficial gut microbes found in animals, along with GA, can inhibit *L. monocytogenes* infection and improve the growth and immunity of host (Bao *et al*., 2019). Navita demonstrated that GA application changes the intestinal microbiota profile, enriching beneficial microbes (Ding *et al*., 2018). However, it requires high concentration of GA for longer durations. GA cannot effectively kill *L. monocytogenes* due to the inactive stationary phase of bacteria and high-density colony-forming units (CFU) (Inada *et al*., 2020; Xu *et al*., 2014). Therefore, it is rare to use GA alone to inhibit pathogenic bacteria.

Currently, the responses of the microbiome and specific bacterial species to *L. monocytogenes*, as well as how UVC-GA acts on this pathogenic bacterium, are still being studied. Therefore, it is crucial to identify an effective treatment to enhance the host's resistance to Listeriosis infection by promoting the diversity and richness of gut microbes. The objective of this study is to examine the alterations in the gut microbiome of *L. monocytogenes*-infected hosts (mice) and assess the impact of UVC-GA on the gut microbiome of these infected hosts.

MATERIALS AND METHODS

The experiment was conducted at the Aquatic Food Processing and Preservation Laboratory of Guangxi Academy of Fishery Sciences (Nanning, Guangxi, China). A mouse model infected with *L. monocytogenes* was created, and this was done by assessing blood parameters and analyzing the bacterial composition of the microbiome (Callahan *et al*., 2016).

Preparation of active L. monocytogenes

The commonly encountered strain of *L. monocytogenes* was obtained from the Guangxi Key Laboratory of the Aquatic Food Processing and Preservation (Guangxi Academy of Fishery Science) and the culture was stored in a glycerin solution at −80°C. At the start of the experiment, the frozen gel was placed in a sterile environment using a sterilized inoculation ring, following which inoculation on blood agar (Qingdao Haibo Bioengineering Company, Qingdao, Shangdong, China), and the plate was incubated at 24°C for 24 h. Typical individual colonies were selected and diluted using sterilized saline and linearly inoculated on blood agar for purification at 37°C for 24 h, and this procedure was repeated three times. Toxicity rejuvenation was conducted according to Gupta *et al*. (2007). To prepare bacterial suspensions, colonies were eluted on blood agar using 0.65% sterilized saline. A bacterial suspension volume of 0.5 mL was intraperitoneally injected into each AC57BL/6 J mouse. Mice were continuously monitored for evidence of disease for one week, during which symptoms of diseased individuals were recorded each day and dead ones were removed and sent to the laboratory. In the laboratory, the dead individuals were assessed for disease symptoms through visceral organs and blood agar was used for pathogen isolation and identification. ThF1: 5′ CTCTCCAATCAATGCCACTTCC 3′ and R1: 5′ CCCTTGTGGAGGTTCCTTGT 3′ diagnostic primer sets were used to verify infection in live individuals and tissues of the gut. Polymerase chain reaction and the settings of the thermal cycler were as outlined in Øvergård *et al*. (2010). Strain purification and culture were administered according to the above approach once *L. monocytogenes* was well affirmed, and bacterial concentration was quantified at a wavelength of 600 mm using an SH-254 spectrophotometer (Shanghai Bioengineering Company, Shanghai, China) according to Rolhion *et al*. (2019). Once

prepared, the stain was immediately used in the infection experiments.

Animal experiment

Experimental protocols were granted by Guangxi Academy of Fishery Science for all animals (Grant number: GAFS2019018). Healthy AC57BL/6 J mouse (n=40, 16-weeks old male and 27.7±1.6 g weight) were purchased from Little Science Biotechnology Limited Company (Nanning, Guangxi, China). Normal mice without infected by *L. monocytogenes* were used as control cohort (CC) (n=10). Infected mice (n=30, 16-weeks old male and 27.7 ± 1.6 g weight) were evenly divided into three cohorts: (1) infected mice (n=10) orally fed with UVC-GA solution were taken as treated cohort (TC); (2) infected mice (n=10) not administered UVC-GA solution were taken as negative cohort (NC); (3) infected mice (n=10) orally fed with GA solution were taken as positive cohort (PC). All mice were reared a normal diet of 10% kcal/fat energy daily, simultaneously orally administered with sterile physiological saline (SPS, 300 µL). All mice were fed at 24 °C and a 12 h light/dark cycle in the animal room equipped with air-condition, and they freely foraged and drunk water. After the mice were acclimated for 7 days, PC- and TC-mice were orally fed with 5 ml/kg body weight UVC-GA or GA, respectively, whereas the CC- and NC-mice were administered SPS using the same strategy. Mice were fed UVC-GA or GA or SPS once a day according to the Km factor ratio of 3 and 37 for 20 g of mice and 60 kg of humans (Reagan *et al*., 2008). The mice were fed the diet twice daily (8:00 and 17:00). Food intake and body weight were recorded other five days, and the experiment period was 20 days.

Sample collection and processing

To investigate the impact of the administration of UVC-GA to the *L. monocytogenes* infected mice, routine sampling was conducted at day 0, 5, 10, 15, and 20 in all four cohorts to measure body weight and gut microbiome. Blood parameters and incidences of mortality in these cohorts were also recorded. Over the four sampling periods, all samples from CC-, NC-, PC- and TC-cohort representing a range of body weight were sequenced for further sample processing. The venous blood (2 mL from each mouse) of the selected mice were aseptically taken using a syringe injected into the bulbous arteriosus. Plasma was isolated from the blood sample using centrifugation at 1,000 *g* for 20 min at 4 °C and the supernatant was stored at −20 °C for subsequent biochemical analysis. The intestinal tract of each sampled mice was obtained using sterile cotton swabs inserted into anal area of 3 cm. Intestinal feces were placed in a 15 mL conical tube. Each swab sample was resuspended in 2 mL of Luria-Bertani broth and 2 mL of 30% glycerol, decanted into three tubes (2 mL) and frozen in an ultra-low temperature freezer at −80°C. All detected trials were done in three replicates.

Measurement of blood parameters of infected mice

The immune proteins to be measured included total protein (TP), immunoglobulin (IgM) and albumin (ALB), and were detected using a fluorescent spectrophotometer (Hitachi Ltd, Japan). Enzyme-linked immunoassay kits were obtained from Nanjing Jiancheng Bioengineering Institute (Nanjing, Jiangsu, China). IgM content in samples was measured by the orderly addition of horseradish peroxidase-labeled detection antibodies (Nanjing Jiancheng Bioengineering Institute) for a reaction of 10 min at room temperature. The substrate tetramethylbenzidine was then added to the above solution and observed for color change at room temperature for 5 min. The absorbed IgM was detected at a wavelength of 450 nm, and the content of IgM was determined by reference to the standard. The bicinchoninic acid method was used to measure TP. A mixture of 20 µL of the sample and 250 µL of bicinchoninic acid was incubated at 37 ℃ for 30 min. Finally, 30% ethanol was added to stop the reaction and the solution was left for 5 min at room temperature. Absorbed TP was then detected at a wavelength of 562 nm. ALB was measured by mixing 10 µL of the sample with 2.5 mL bromocresol green reagent, and the mixture was allowed to stand at room temperature for 10 min. ALB content was then measured at a wavelength of 628 nm.

Extraction and amplification of DNA and gene sequencing of 16S rRNA

DNA from intestinal cells of individual mice was collected using CTAB/phenol: Chloroform extraction as according to Xu *et al*. (2014). Molecular grade water was used to precipitate DNA, following which the DNA was fluorometrically quantified. The quality of DNA was analyzed through absorbance measurement at a wavelength of 260 nm with the use of a NanoDrop spectrophotometer (Thermo Scientific). Dilution of intestinal DNA to 1 ng μL^{-1} was implemented, following which it was transferred to two 96-well plates. Indexing primers and the one-step custom PCR protocol was used to generate the Amplicon libraries as outlined in Kozich *et al*., (2013) and the 341F: (5′ CCTAYGGGRBGCASCAG 3′) and 806B (5′ GGACTACNVGGGTWTCTAAT 3′) V4 primers. Amplification of all samples was conducted in triplicate to minimize PCR bias. The reactions were composed of 30 µL NEBNext PCR mix (New England BioLabs), 3 µL of forward and reverse primers (10 µM), 2 µL H_2O and 10 µL of template DNA (1 ng/µL). Initial denaturation was

conducted at 98 °C for 1 min, after which 30 cycles of denaturation for 10 s at 98 °C, 30 s of annealing at 50 °C and 30 s of extension at 72 °C was implemented. The final extension was conducted at 72 °C for 5 min. Triplicate PCR reactions were then pooled prior to purification.

Agenourt AMPure XP bead-based clean-up was used to purify amplicon libraries to remove primer dimers and free primers. After resuspension of the cleaned DNA in a buffer (Illumina), an assessment of length of the amplicon was implemented using the D1000 Screen Tape system (Agilent). A fragment size of approximately 400 bp was expected. The Promega Glomax kit was used to quantify libraries. Two independent library pools were made in consideration of the low yield of certain libraries. After dilution to 2 µM, these were mixed according to their ratio share of the samples. Determination of the concentration of the final pool was through quantitative PCR. Sequencing was conducted using 196 libraries, including two controls, 250 bp reads (v2 chemistry) and the Illumina Miseq Illumina HiSeq platform (Beijing Novogene Bio-information Science and Technology Co., Ltd., China). Raw reads were deposited in the National Center for Biotechnology Information (NCBI) sequence read archive under the BioProject PRJNA577421.

Bioinformatics analysis

The R DADA2 analysis package was used to process all reads (Callahan *et al*., 2016). Trimming of paired-end reads was according to visualized scores of quality and standard filtering parameters of DADA2's: maxN= 2, truncQ= 2, rm. phix= TRUE, and maxEE= 2. The parametric error model of DADA2 was fitted using the initial 1×10^8 bases. Sequences were de-replicated and inference of sequence variants was achieved using pseudo-pooling and the associated error model. Merged filtered reads were applied to build the table of amplicon sequence variants. Trimming and removal of chimeras was then implemented on the denoised full length sequences. The Silva database (v.132) was used to assign taxonomy. The run accuracy was measured using a mock community of known samples sequenced with a negative control. No measurable DNA was contained in the negative control library and it produced more than 2% of sequences compared to the average read count.

The basic local alignment search tool was used to compare all reads with the full nr database using the DIAMOND v0.7.9 blastx function (Buchfink *et al*., 2015). Classified reads were visualized in MEGAN6 Community Edition v6.5.5 (Huson *et al*., 2016) and sequences not representing bacteria were removed. Non-applicable taxonomic assignments were labeled using the lowest characterized taxonomic rank. Matrices of alpha diversity were analyzed within the phyloseq package (McMurdie *et al*., 2013). Pruning of exact sequence variants (ESVs) was conducted before non-metric multidimensional scaling; ESVs not found in at least one sample were removed along with samples with more than 1,000 reads. Seed were set at 2,209. The packages Phyloseq and ggplot2 were used to visualize taxonomic profiles and diversity measures. The rgl package was used to visualize three-dimensional ordinations (Adler *et al*., 2003).

Statistical analyses

Each experiment has three replicates and the R statistical environment was used to conduct statistical analyses (R Core Team, 2011). Assessment of the normal distribution of variables was conducted using the Shapiro–Wilk's test with the Shapiro test function. Before downstream analysis, non-normal values were log-transformed. A small numeric constant (half of the detection limit: 0.00003661) was added to all values before logarithm transformation to quantify the relative abundance of specific bacterial taxa not present in samples. Variation in the dataset was correlated using linear models containing interaction terms. Running of Permutational multivariate analysis of variance was through the adonis function of in the Vegan software package. The same package was used to calculate the multivariate homogeneity of group dispersions (Betadisper). A total of 999 permutations were used in both aforementioned analyses (Oksanen *et al*., 2013).

RESULTS

The model of L. monocytogenes *infected mice*

Infected mice observed of 0–25 days showed symptoms of infection such as reduced appetite, abnormal movements, fully filled ascites in the abdominal cavity and larger liver size. The blood parameter measurements showed lower TP, IgM and ALB in the CGs over 25 days compared to the CC (healthy individuals of 0 day) (Fig. 1A, B, C), which confirmed viral infection in mice. The results indicated that the model of *L. monocytogenes* infected individuals was accurate, as reported by Harvey *et al*. (2007) and Guo *et al*. (2016).

Small-subunit (SSU)

A total of 11,254,317 bacterial ribosomal small-subunit (SSU) reads from the V4 region from 483 samples were left after filtering. Each sample was on average represented by 22,947±1,054 reads. Sequencing depth ranged from 1,167–162,489 reads across all samples. values exceeding 0.975 were obtained for the good's coverage index in all filtered samples, showing that more

than 2% of reads in each sample appear only once (Fig. 2A) and near-saturation of community coverage was indicated by rarefaction curves (Fig. 2B). However, singletons were only kept if they were in multiple samples so as to remove artefactual sequences. The SSU indicated that the data of samples could use to gut microbiome analysis.

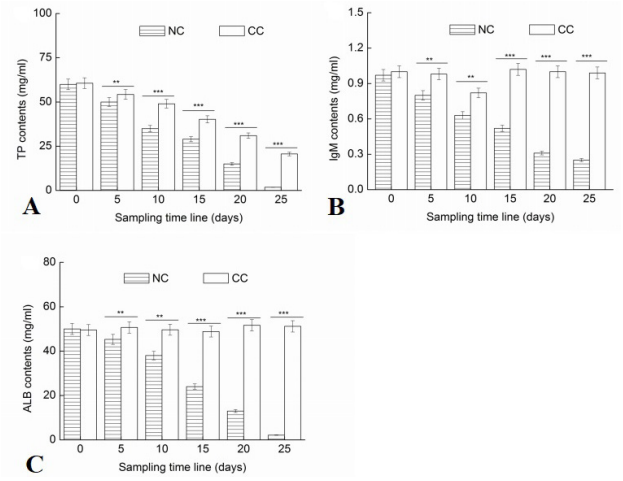

Fig. 1. The contents of immune proteins of animals for 25 days when as they were fed with combined probiotics. Immune proteins: A: TP, total protein; B: IgM, immunoglobulin; C: ALB, albumin. CC, mice were not administrated any UVC-GA solution and infected by *L. monocytogenes* as control cohort; NC, infected mice was not administered by UVC-GA solution as a negative cohort. Various letters represent significant difference among groups. Error bars indicate the mean and standard deviation (n= 3), $^{**}p < =0.01$, $^{***}p < =0.001$.

Gut microbiome profile of mice

The ESVs of *Listeria* spp. identified in all TCs and all NCs increased over time, and those in the NCs were higher. How, there was not detected in CC. The ESVs of genera *Enterococcus*, *Synechococcus*, *Prevotella*, *Roseovarius*, *Psychromonas, Clostridium,* and *Bacillus* were detected in TCs and CC, whereas no detection of these was determined in NCs. For each of the genera *Enterococcus*, *Synechococcus*, *Prevotella*, and *Bacillus*, no significant difference in the ESV numbers between TCs and CC was found, whereas the ESVs of the genera *Roseovarius*, *Psychromonas*, and *Clostridium* in CC were higher than those of all TCs. Although there was detection of lower ESVs of *Lactobacillus* spp. and *Photobacterium* spp. in average profiles at 5–25 days in the NCs, it comprised substantial proportions of profiles in the TCs post oral administration. ESVs numbering 20 under this assignment of *Lactobacillus* spp. and *Photobacterium* spp. were shared across all TC profiles. In addition, sequence

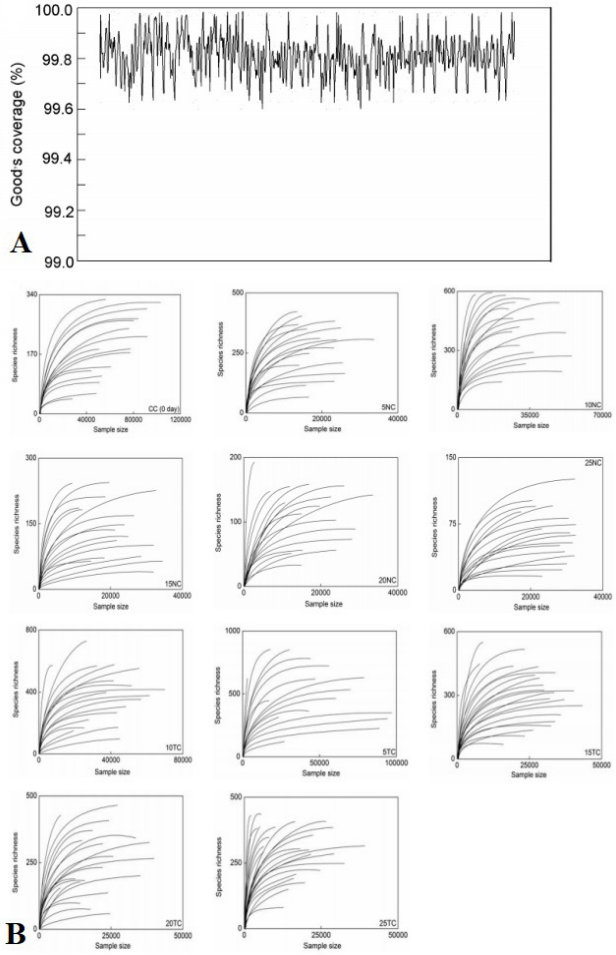

Fig. 2. Sequencing coverage across all samples. Estimations of community saturation across all individuals. A: Goods coverage estimates. B: Rarefaction of increasing sequencing effort. Plots colored according to sample group. Time increases towards to extremities of the x axis from 0 week to end (25 days).

variants were aligned with these two genera in the Silva database with relatively low identity, ranging from 64.6% to 96.4%. For each of *Psychrilyobacter* spp., *Phascolarctobacterium* spp., and *Vibrio* spp., no significant difference in ESVs among them was obtained. However, in NCs, the ESVs of both genera *Psychrilyobacter* and *Vibrio* were detected at the first two sampling time points, and the ESVs of *Phascolarctobacterium* spp. was only found at 5 days. The ESVs of *Bifidobacterium* and *Bacteroides* genera in all TCs and CCs were higher than those of NCs. Although the ESVs of two genera in TCs was less than 20, it still comprised substantial proportions of profiles in the TCs post oral administration. In addition, there was not detection of *Bifidobacterium* spp. and *Bacteroides* spp. at final sampling

time points. For *Carboxylicivirga* spp., it was not found in CC, NCs and TCs over sampling time, and no significant difference among them. Meanwhile, the *Streptococcus* genus was only detected in NC at 10 days (Fig. 3A, B, C and Table I). In total, there was more ESVs and genera in TCs compared to the NCs, and they were close to those of CC.

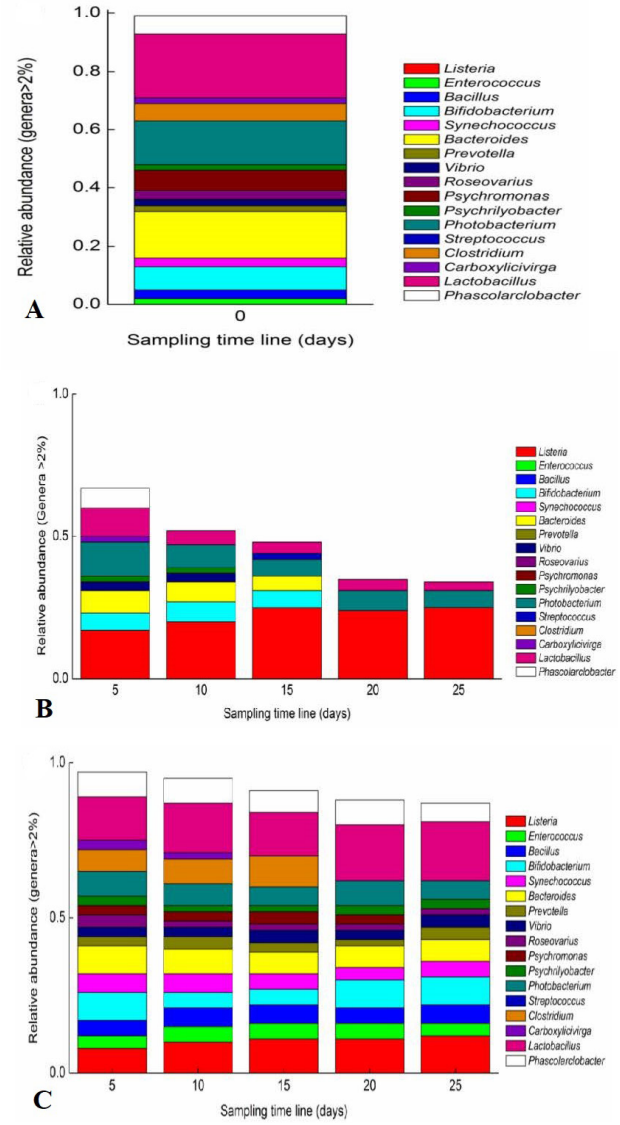

Fig. 3. Average bacterial profiles of all animals sampled over 25 days. Bacterial genera representing more than 1% of entire 16S community. Genera coloured according to key. Time increases towards to extremities of the x axis from 0 week to end (25 days) at the bottom. A: CC, mice were not administrated any UVC-GA solution and infected by *L. monocytogenes* as control cohort. B: NC, infected mice were not administered by UVC-GA solution as a negative cohort. C: TC, infected mice were orally fed with UVC-GA solution as treated cohort.

Table I. Exact sequence variant count of bacterial genera representing > 2% relative abundance.

Genus	Number of exact sequence variants (ESVs)										
	NC (day)					CC (day)	TC (day)				
	25	**20**	**15**	**10**	**5**	**0**	**5**	**10**	**15**	**20**	**25**
Listeria	25	24	25	20	17	-	8	10	11	11	12
Enterococcus	-	-	-	-	-	5	4	5	5	5	4
Bacillus	-	-	-	-	-	6	5	6	6	5	6
Bifidobacterium	-	-	6	7	6	13	11	10	10	9	9
Synechococcus	-	-	-	-	-	6	6	6	5	4	5
Vibrio	-	-	-	3	3	3	3	3	4	3	4
Bacteroides	-	-	5	7	8	18	15	11	12	14	12
Prevotella	-	-	-	-	-	3	3	4	3	2	4
Roseovarius	-	-	-	-	-	6	4	2	2	2	2
Psychromonas	-	-	-	-	-	7	3	3	4	3	-
Psychrilyobacter	-	-	-	2	2	2	3	2	2	3	3
Photobacterium	6	7	6	8	12	20	18	16	14	15	16
Streptococcus	-	-	2	-	-	-	-	-	-	-	-
Clostridium	-	-	-	-	-	11	7	8	10	-	-
Carboxylicivirga	-	-	-	-	2	2	3	2	-	-	-
Lactobacillus	3	4	4	5	10	22	16	18	16	20	21
Phascolarclo-bacterium	-	-	-	-	7	8	8	8	7	8	6

Bacterial richness (Chao1) and diversity (Shannon index) of the mice gut microbiome

The species richness (Chao1) and species diversity (Shannon's diversity) averages of the gut biome were significantly higher in mice from the TC groups compared to NC groups (Chao1; P-value < 0.001. Shannon's; P-value < 0.001). A linear model showed a significant loss in bacterial richness or diversity over time in the NCs, whereas in the TCs, species richness remained relatively constant with time (Chao1; P-value < 0.001. Shannon's; P-value < 0.001) (Fig. 4A, B). It should be noted that an analysis of the results of the linear model shows that the NCs with no UVC-GA and TCs with UVC-GA explain all variability found in the data.

Survival rate

The survival curve of *L. monocytogenes* infected mice after 25 days showed the survival rate to be zero in the NCs within 10 days, whereas that of the TCs was > 60%, and survival in the TC groups showed an upward trend compared with the NC (Fig. 5). The results show that UVC-GA could effectively improve the survival of mice after infection with *L. monocytogenes*.

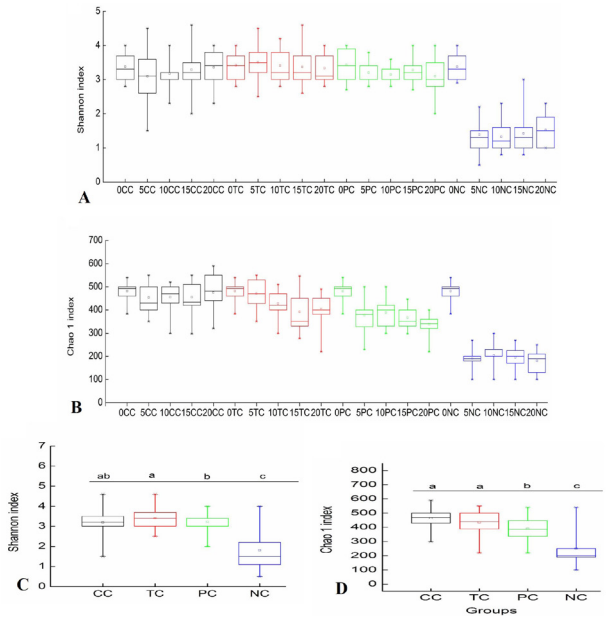

Fig. 4. Alpha diversity measures of all sample groups. A: Shannon's measure of species diversity across all sampling time time. B: Chao1 estimate of species richness across all sampling time time. C: Shannon's measure of species diversity across four groups. D: Chao1 estimate of species richness across four groups. NC, infected mice was not administered by UVC-GA solution as a negative cohort; TC, infected mice was orally fed with UVC-GA solution as treated cohort. Significant difference among groups was marked using different letters. Error bars indicate the mean and standard deviation (n= 3) , $p < =0.05$.

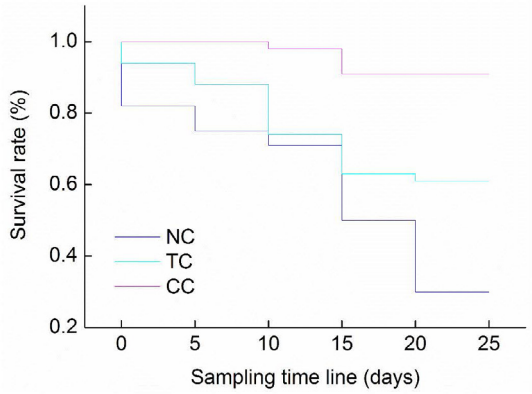

Fig. 5. Survival curve of mice with infection of *L. monocytogenes* for 25 days of culture when as mice were fed with UVC-GA solution. CC, Mice were not administrated any UVC-GA solution and infected by *L. monocytogenes* as control cohort; NC, infected mice was not administered by UVC-GA solution as a negative cohort; TC, infected mice was orally fed with UVC-GA solution as treated cohort.

DISCUSSION

The current research demonstrated that the microbial richness and diversity of the gut biomes of virus-infected mice were reduced compared to those of healthy individuals as the infection compromised intestinal structure and reduced appetite, thereby disrupting the homeostasis of the gut microbiome, and resulting in the disappearance of certain bacterial taxa (Nohynek *et al*., 2006). Bacterial infection correlates with dynamic changes in the microbial richness and diverse the gut microbiome, which ultimately impacts the growth of the hos (Nohynek *et al*., 2006). Several studies have claimed that bacterial diversity changes in the gut microbiome correlate with changes in the health of the host and incidences of enteric disease (Garcia-Gutierrez *et al*., 2019). The antagonistic potential within a microbiome with high bacterial diversity can perhaps increase pathogen resistance and could reduce microbiome susceptibility to incoming pathogens, thereby preventing the establishment of infection (Donaldson *et al*., 2016). A reduction in the diversity of the gut microbiome and the subsequent compromise of the ability of the microbiome to resist incoming pathogens could allow the proliferation of enteric pathogens such as *L. monocytogenes* (Garcia-Gutierrez *et al*., 2019). *L. monocytogenes* can colonize the host through the digestive tract, relying on entering through the intestinal epithelia (Rolhion *et al*., 2019). A possible explanation for the bacteria not being detected in CC mice whereas the virus proliferated NCs is that the diversity of the gut microbiome of mice in the NCs was compromised, and this impacted the gut microbiome's resistance to colonization by the bacteria and subsequent infection. At the same time, all the mice in the NC group died, which was consistent with the low infection rate but high mortality of intestinal infection caused by *L. monocytogenes*. Furthermore, *L. monocytogenes* infection and the associated compromise of host immunity may result in lowered host selection pressures within the gut and result in the observed variations in the diversity and richness of the microbiota.

The results of the present study showed significant differences in the composition of gut microbiota between the NC and TC groups, and while *L. monocytogenes* dominated the NC groups by impeding other bacteria. The gut microbiota profiles in the TC groups were improved by the oral administration of UVC-GA solution. The colonization and infection by the bacteria are dependent on microbes present in the gut, and the diversity and species richness of the gut microbiome can account for differences in the resistance of individuals in a population to bacterial infection and may explain the higher incidence of bacterial infection in aged individuals (Rhoades *et al*., 2019; Sadiq, 2020).

Several genera attracted our attention, such as *Vibrio* spp. The *Vibrio* genus is often reported as the predominant genus found in the gut microbiomes of animals (Kim *et al*., 2019; Suginta *et al*., 2000). Several *Vibrio* spp. are well known to be human pathogens. As an example, *Vibrio harveyi* infection can disrupt the digestive tract epidermal tissue of organisms (Lee *et al*., 2015; Austin and Zhang, 2006). The observation of fewer ESVs of the *Vibrio* genus in TCs compared to NCs groups may be because the beneficial *Vibrio* genus was inhibited by the virus *L. monocytogenes*, and the oral administration of UVC-GA solution in the diet of infected mice resulted in the introduced microorganism outcompeting the *Vibrio* genus in the capture of nutrients and thereby impeded *Vibrio* reproduction.

The genera *Photobacterium* and *Lactobacillus* were identified from the gut of animals, and they are thought that it has a symbiotic relationship with dace by facilitating these animals to survive on the food of low quality (Xu *et al*., 2014). The foods of dace are predominantly of low nutrients such as decaying plant matter, and therefore a symbiotic association allowing them to more efficiently sequester nutrition from ingested food would benefit them. It is confirmed that these sorts of symbiotic relationships may have allowed dace to colonize terrestrial environments as these bacteria have also been found in the gut of other animals (Xiong *et al*., 2017), for example, this bacteria was also found in the cow. An interesting result is that considerable amounts detected in TCs in the current study were also found in NCs, implying a competitive relationship between *L. monocytogenes* and this bacterial species. Furthermore, this implies that *Photobacterium* and *Lactobacillus* may outcompete *L. monocytogenes* for intestinal tract nutrients. An additionally observed phenomenon was that the oral administration of UVC-GA solution could maintain considerable levels of the two bacterial species.

Many of the species in the large family *Bacteroides* and *Bifidobacterium* are important animal bacteria (Sugahara *et al*., 2015; Ceccaldi, 1989). The ESVs detected in the present study that was annotated as *Bacteroides* match several bacteria isolated from the microbiomes of human (Brook, 1989). *Bacteroides* have been identified in humans afflicted with the commonly-occurring bacterium that result in damage to the respiratory passage in the body (Brook, 1989). *Bifidobacterium* was identified in the gut microbiome of mice in the present study, and it was detected in all TC groups but only in NCs at 20-15 days. The presence of higher amounts of these genera in the CC compared to the TC groups might be because infection by *L. monocytogenes* and/or the oral administration of UVC-GA solution has no bearing on the presence of this genus. More research is needed to determine why this genus disappears in the NC groups over time.

The genera *Phascolarctobacterium* and *Carboxylicivirga* comprised considerable substantial fractions of the microbiomes of infected mice in the NC groups at 5 days. The *Carboxylicivirga* ESV is very similar to those of clones of *Roseobacter* associated with toxic algal blooms (KY277241 and KY277569), and those identified in the human gut (Wang *et al*., 2015). However, the function of this relatively recently recognized genus in any of its host species remains largely unknown (Zhang *et al*., 2016). Several *Phascolarctobacterium* species have been related to particular animal species, and have been identified in both humans and mice. In addition, multiple species are recognized as emerging pathogens of animals and have been linked to intestinal disease (Tran *et al*., 2019; Wu *et al*., 2017). The ESVs assigned to *Phascolarctobacterium* identified from the gut microbiomes of mice matched those isolated from the gut microbiomes of humans (Tran *et al*., 2019). The oral administration of UVC-GA solution restrained the colonization of the *Phascolarctobacterium* in TC-mice over time, but the *Carboxylicivirga* disappeared. and this observation could be explained by the *Carboxylicivirga* genera were sensitive to the UVC-GA solution.

For some diseases, the health of the host and the incidence of the disease is related to changes in the species diversity and richness of the gut microbiome, and the administration of microorganisms in the diet can improve bacterial species richness and diversity within the gut tract, thereby increasing the commensal bacterial community and the production of antimicrobial peptides, stimulating the host immune system and ultimately affecting the resistance of the host to other potential pathogenic microbes in the gut (Donaldson *et al*., 2016; Garcia-Gutierrez *et al*.,2019). GA can inhibit a variety of planktonic bacteria, biofilms, and fungi via produce ROS and decompose bacterial membranes (Nohynek *et al*., 2006; Nakamura *et al*., 2015). Administration of GA can improve gut bacteria richness and diversity, consequently promoting the microbiome health and host immune system stimulation, and ultimately increasing the host's tolerance to other microbes in the gut (Gupta *et al*., 2007). Previous studies also have shown that animals who have been administered GA maintained a low incidence of *L. monocytogenes* infection by greater species diversity and richness of the gut microbiome, which improved the resistance of the gut microbiome to virus colonization (McMurdie and Holmes, 2013). The immunity of a host to *L. monocytogenes* infection can be enhanced by improving the species richness and diversity of the gut microbiome, which provides an increase in host selection pressures (Becattini *et al*., 2017). In the present

study, the TC groups showed greater bacterial species richness and diversity in the gut microbiome of infected mice compared to the NC groups. A possible explanation for this is that the higher bacterial species diversity and richness in the gut microbiomes of mice in the TC group resulting from the administration of GA irradiated by UV-C enhanced the resistance of the mice to *L. monocytogenes* infection by increasing selection pressures and inhibiting the proliferation and establishment of this enteric pathogen. However, it is essential to investigate whether the effectiveness of UVC-GA is higher than GA.

The results of the current study show how *L. monocytogenes* infection in mice can correlate with changes to the gut microbiome and how the oral administration of UVC-GA solution can enhance the ability of infected individuals to resist this infection by strengthening the gut microbiome. The high blood parameters detected in the CC-mice compared to the NC demonstrates the accuracy of the model of *L. monocytogenes* infected individuals constructed in the present study. Results showed that the gut microbiome of infected mice improved through the oral administration of UVC-GA solution. Infected mice that were orally administered UVC-GA solution had more microbially rich and diverse microbiomes of the gut, in contrast to infected individuals in the NC in which the UVC-GA solution was not administered. Therefore, the administration of UVC-GA solution to fed mice could potentially enhance the resistance against *L. monocytogenes*. Also, this study indicated that the UVC-GA solution could be applied as a potential probiotic for beneficial microorganisms.

Furthermore, extended monitoring with increased numbers of samples is a prerequisite for analyzing the relationship between *L. monocytogenes* infection and the gut microbiome of mice under the administration of UVC-GA solution, to confirm the observations of the current study. Transcriptomic or metagenomic analysis can provide more clarity on the potential of administration of UVC-GA solution to the normal diet of mice for changing the phylogenetic community structure and host metabolic processes. Considered collectively, this knowledge could be applied to the design of new and effective potential probiotics for beneficial microorganisms to improve the cultivation of their species. However, the effective dosage and time needs to be further investigated.

DECLARATIONS

Acknowledgments

This project was funded by Science and Technology Fund of Guangxi Province (AB16380074), Science and Technology Major Project of Guangxi (AB21196020), the Guangxi key R & D projects (AB19245013), and National Natural Science Foundation of China (81960164). We also thank Philip Creed, PhD for editing the English text of a draft of this manuscript.

Funding

The Major Science and Technology Fund of Guangxi Province (AB21220048, AB23026063 and AB23026134). National Natural Science Foundation (32360628).

IRB approval

The research project was approved by the Guangxi Academy of Fishery Sciences, Guangxi, China.

Ethics statement

All the rules and regulations approved by ethical committee of Fishery Breeding and Processing Research Laboratory were followed.

Data availability

All data generated or analyzed during this study are included in this published article.

Statement of conflict of interest

The authors have declared no conflict of interest.

REFERENCES

Adler, D., Nenadić, O. and Zucchini, W., 2003. *RGL: A R-library for 3D visualization with OpenGL*. http://rgl.neoscientists.org/arc/doc/RGL_INTERFACE03.pdf.

Austin, B. and Zhang, X.H., 2006. *Vibrio harveyi*: A significant pathogen of marine vertebrates and invertebrates. *Lett. appl. Microbiol*., **43**: 119-124. https://doi.org/10.1111/j.1472-765X.2006.01989.x

Bao, T., Li, Y., Xie, J., Jia, Z. and Chen, W., 2019. Systematic evaluation of polyphenols composition and antioxidant activity of mulberry cultivars subjected to gastrointestinal digestion and gut microbiota fermentation. *J. Funct. Fds*., **58**: 338-349. https://doi.org/10.1016/j.jff.2019.05.017

Becattini, S., Littmann, E.R., Carter, R.A., Kim, S.G., Morjaria, S.M., Ling, L., Gyaltshen, Y., Fontana, E., Taur, Y., Leiner, I.M. and Pamer, E.G., 2017. Commensal microbes provide first line defense against Listeria monocytogenes infection. *J. exp. Med*., **214**: 1973-1989. https://doi.org/10.1084/jem.20170495

Bernbom, N., Licht, T.R., Saadbye, P., Vogensen, F.K. and Nørrung, B., 2006. *Lactobacillus plantarum* inhibits growth of *Listeria monocytogenes* in an

in vitro continuous flow gut model, but promotes invasion of *L. monocytogenes* in the gut of gnotobiotic rats. *Int. J. Fd. Microbiol*., **108**: 10-14. https://doi.org/10.1016/j.ijfoodmicro.2005.10.021

Brook, I., 1989. Direct and indirect pathogenicity of beta lactamase producing bacteria in mixed infections in children. *Crit. Rev. Microbiol*., **16**: 161-180. https://doi.org/10.3109/10408418909104470

Buchfink, B., Xie, C. and Huson, D.H., 2015. Fast and sensitive protein alignment using Diamond. *Nat. Methods,* **12**: 59-60. https://doi.org/10.1038/nmeth.3176

Callahan, B.J., McMurdie, P.J., Rosen, M.J., Han, A.W., Johnson, A.J. and Holmes, S.P., 2016. DADA2: High-resolution sample inference from *Illumina amplicon* data. *Nat. Methods*, **13**: 581-583. https://doi.org/10.1038/nmeth.3869

Ceccaldi, H.J., 1989. Anatomy and physiology of digestive tract of crustaceans decapods reared in aquaculture. *Actes de Colloque,* **9**: 243-259. https://archimer.ifremer.fr/doc/00000/1486/

Cossu, A., Ercan, D., Wang, Q., Peer, W.A., Nitin, N. and Tikekar, R.V., 2016. Antimicrobial effect of synergistic interaction between UV-A light and gallic acid against *Escherichia coli* O157:H7 in fresh produce wash water and biofilm. *Innov. Fd. Sci. Emerg. Technol*., **37**: 44-52. https://doi.org/10.1016/j.ifset.2016.07.020

Ding, Q., Alborzi, S., Bastarrachea, L.J. and Tikekar, R.V., 2018. Novel sanitization approach based on synergistic action of UV-A light and benzoic acid: Inactivation mechanism and a potential application in washing fresh produce. *Fd. Microbiol*., **72**: 39-54. https://doi.org/10.1016/j.fm.2017.11.004

Donaldson, G.P., Lee, S.M. and Mazmanian, S.K., 2016. Gut biogeography of the bacterial microbiota. *Nat. Rev. Microbiol*., **14**: 20-32. https://doi.org/10.1038/nrmicro3552

Garcia-Gutierrez, E., Mayer, M.J., Cotter, P.D. and Narbad, A., 2019. Gut microbiota as a source of novel antimicrobials. *Gut Microb*., **10**: 1-21. https://doi.org/10.1080/19490976.2018.1455790

Guo, A., Xu, Y., Mowery, J., Nagy, A., Bauchan, G., Nou, X., 2016. Ralstonia insidiosa induces cell aggregation of *Listeria monocytogenes*. *Fd. Contr*., **67**: 303-309. https://doi.org/10.1016/j.foodcont.2016.03.006

Gupta, N., Gupta, S. and Mahmood, A., 2007. Gallic acid inhibits brush border disaccharidases in mammalian intestine. *Nutr. Res*., **27**: 230-235. https://doi.org/10.1016/j.nutres.2007.02.001

Harvey, J., Keenan, K.P. and Gilmour, A., 2007. Assessing biofilm formation by *Listeria monocytogenes* strains. *Fd. Microbiol*., **24**: 380-392. https://doi.org/10.1016/j.fm.2006.06.006

Huson, D.H., Beier, S., Flade, I., Górska, A., El-Hadidi, M., Mitra, S., Ruscheweyh, H.J. and Tappu, R., 2016. Megan community edition- interactive exploration and analysis of large-scale microbiome sequencing data. *PLoS Comput. Biol*., **12**: e1004957. https://doi.org/10.1371/journal.pcbi.1004957

Inada, K.O.P., Silva, T.B.R., Lobo, L.A., Domingues, R.M.C.P., Perrone, D. and Monteiro, M., 2020. Bioaccessibility of phenolic compounds of jaboticaba (*Plinia jaboticaba*) peel and seed after simulated gastrointestinal digestion and gut microbiota fermentation. *J. Funct. Fds*, **67**: 103851. https://doi.org/10.1016/j.jff.2020.103851

Kim, K.I., Won, K.M., Lee, E.S., Cho, M., Jung, S.H. and Kim, M.S., 2019. Detection of vibrio and ten vibrio species in cage-cultured fish by multiplex polymerase chain reaction using house-keeping genes. *Aquaculture*, **506**: 417-423. https://doi.org/10.1016/j.aquaculture.2019.03.073

Kozich, J.J., Westcott, S.L., Baxter, N.T., Highlander, S.K., Schloss, P.D., 2013. Development of a dual-index sequencing strategy and curation pipeline for analyzing amplicon sequence data on the MiSeq Illumina sequencing platform. *Appl. Environ. Microbiol*., **79**: 5112-5120. https://doi.org/10.1128/AEM.01043-13

Lagier, E., Staumont, G., Tubery, M., Didier, A., Rouquette, I. and Frexinos, J., 1996. Specific respiratory manifestations associated with ulcerative colitis. A case report and review of the literature. *Gastroenterolo. Clini. et Biolog.,* **20**: 397-400.

Lawley, T.D. and Walker, A.W., 2013. Intestinal colonization resistance. *Immunology*, **138**: 1-11. https://doi.org/10.1111/j.1365-2567.2012.03616.x

Lee, C.T., Chen, I.T., Yang, Y.T., Ko, T.P., Huang, Y.T., Huang, J.Y., Huang, M.F., Lin, S.J., Chen, C.Y., Lin, S.S., Lightner, D.V., Wang, H.C., Wang, A.H.J., Wang, H.C., Hor, L.I. and Lo, C.F., 2015. The opportunistic marine pathogen *Vibrio parahaemolyticus* becomes virulent by acquiring a plasmid that expresses a deadly toxin. *Proc. natl. Acad. Sci.,* **112**: 10798-10803. https://doi.org/10.1073/pnas.1503129112

McMurdie, P.J. and Holmes, S., 2013. Phyloseq: An R package for reproducible interactive analysis and graphics of microbiome census data. *PLoS One*, **8**: e61217. https://doi.org/10.1371/journal.pone.0061217

Nakamura, K., Ishiyama, K., Sheng, H., Ikai, H., Kanno, T. and Niwano, Y., 2015. Bactericidal activity and mechanism of photoirradiated polyphenols against gram-positive and -negative bacteria. *J. Agric. Fd. Chem*., **63**: 7707-7713. https://doi.org/10.1021/jf5058588

Nohynek, L.J., Alakomi, H.L., Kähkönen, M.P., Heinonen, M., Helander, I.M., Oksman-Caldentey, K.M. and Puupponen-Pimiä, R.H., 2006. Berry phenolics: Antimicrobial properties and mechanisms of action against severe human pathogens. *Nutr. Cancer*, **54**: 18-32. https://doi.org/10.1207/s15327914nc5401_4

Oksanen, J., Blanchet, F.G., Kindt, R., Legendre, P., Minchin, P., O'Hara, R.B., Simpson, G., Solymos, P., Stevens, M.H.H. and Wagner, H., 2013. *Vegan: Community ecology package. R package version*. 2.0-10. CRAN 2013. https://github.com/vegandevs/vegan

Øvergård, A.C., Nerland, A.H. and Patel, S., 2010. Evaluation of potential reference genes for real time RT-PCR studies in Atlantic halibut (*Hippoglossus hippoglossus* L.); during development, in tissues of healthy and NNV-injected fish, and in anterior kidney leucocytes. *BMC Mol. Biol*., **11**: 36. http://www.biomedcentral.com/1471-2199/11/36 https://doi.org/10.1186/1471-2199-11-36

Reagan-Shaw, S., Nihal, M. and Ahmad, N., 2008. Dose translation from animal to human studies revisited. *FASEB J. Off. Publ. Feder. Am. Soc. exp. Biol*., **22**: 659-661. https://doi.org/10.1096/fj.07-9574LSF

Ren, Y., Liu, H., Liu, X., Zheng, Y., Li, Z., Li, C., Yeung, K.W.K., Zhu, S., Liang, Y., Cui, Z. and Wu, S.L., 2020. Photoresponsive materials for antibacterial applications. *Cell Rep. Phys. Sci*., **1**: 100245. https://doi.org/10.1016/j.xcrp.2020.100245

Rhoades, N., Mendoza, N., Jankeel, A., Sureshchandra, S., Alvarez, A.D., Doratt, B., Heidari, O., Hagan, R., Brown, B., Scheibel, S., Marbley, T., Taylor, J. and Messaoudi, I., 2019. Altered immunity and microbial dysbiosis in aged individuals with long-term controlled HIV infection. *Front. Immunol*., **10**: 463. https://doi.org/10.3389/fimmu.2019.00463

Rolhion, N., Chassaing, B., Nahori, M.A., de Bodt, J., Moura, A., Lecuit, M., Dussurget, O., Bérard, M., Marzorati, M., Fehlner-Peach, H., Littman, D.R., Gewirtz, A.T., Van de Wiele, T. and Cossart, P., 2019. A listeria monocytogenes bacteriocin can target the commensal prevotella copri and modulate intestinal infection. *Cell Host Microb*, **26**: 691-701. e695. https://doi.org/10.1016/j.chom.2019.10.016

Rouquette, C. and Berche, P., 1996. The pathogenesis of infection by *Listeria monocytogenes*. *Microbiologia*, **12**: 245-258. https://pubmed.ncbi.nlm.nih.gov/8767708/

Sadiq, F.A., 2021. Is it time for microbiome-based therapies in viral infections? *Virus Res*., **291**: 198203. https://doi.org/10.1016/j.virusres.2020.198203

Sallami, L., Marcotte, M., Naim, F., Ouattara, B., Leblanc, C. and Saucier, L., 2006. Heat inactivation of Listeria monocytogenes and *Salmonella enterica* serovar Typhi in a typical bologna matrix during an industrial cooking-cooling cycle. *J. Fd. Prot*., **69**: 3025-3030. https://doi.org/10.4315/0362-028X-69.12.3025

Sanhueza, L., Melo, R., Montero, R., Maisey, K., Mendoza, L. and Wilkens, M., 2017. Synergistic interactions between phenolic compounds identified in grape pomace extract with antibiotics of different classes against *Staphylococcus aureus* and *Escherichia coli*. *PLoS One*, **12**: e0172273. https://doi.org/10.1371/journal.pone.0172273

Sugahara, H., Odamaki, T., Fukuda, S., Kato, T., Xiao, J.Z., Abe, F., Kikuchi, J. and Ohno, H., 2015. Probiotic *Bifidobacterium longum* alters gut luminal metabolism through modification of the gut microbial community. *Sci. Rep*., **5**: 13548. https://doi.org/10.1038/srep13548

Suginta, W., Robertson, P.A., Austin, B., Fry, S.C., Fothergill-Gilmore, L.A., 2000. Chitinases from vibrio: Activity screening and purification of chiA from *Vibrio carchariae*. *J. appl. Microbiol*., **89**: 76-84. https://doi.org/10.1046/j.1365-2672.2000.01076.x

Theivagt, A.E. and Friesen, J.A.J.T.F.J., 2006. *Purification and characterization of* Listeria monocytogenes *HMG-CoA Reductase*. pp. 20. https://doi.org/10.1096/fasebj.20.4.A472-b

Tran, T.T.T., Cousin, F.J., Lynch, D.B., Menon, R., Brulc, J., Brown, J.R.M., O'Herlihy, E., Butto, L.F., Power, K., Jeffery, I.B., O'Connor, E.M. and O'Toole, P.W., 2019. Prebiotic supplementation in frail older people affects specific gut microbiota taxa but not global diversity. *Microbiome*, **7**: 39. https://doi.org/10.1186/s40168-019-0654-1

Wang, F.Q., Zhou, Y.X., Lin, X.Z., Chen, G.J., Du, Z.J., 2015. *Carboxylicivirga linearis* sp. nov., isolated from a sea cucumber culture pond. *Int. J. Syst. Evol. Microbiol*., **65**: 3271-3275. https://doi.org/10.1099/ijsem.0.000407

Wang, Q., de Oliveira, E.F., Alborzi, S., Bastarrachea, L.J. and Tikekar, R.V., 2017. On mechanism behind UV-A light enhanced antibacterial activity of gallic acid and propyl gallate against *Escherichia*

coli O157:H7. *Sci. Rep*., **7**: 8325. https://doi.org/10.1038/s41598-017-08449-1

Wu, F., Guo, X., Zhang, J., Zhang, M., Ou, Z. and Peng, Y., 2017. *Phascolarctobacterium faecium* abundant colonization in human gastrointestinal tract. *Exp. Ther. Med*., **14**: 3122-3126. https://doi.org/10.3892/etm.2017.4878

Xiong, J., Dai, W., Zhu, J., Liu, K., Dong, C. and Qiu, Q., 2017. The underlying ecological processes of gut microbiota among cohabitating retarded, overgrown and normal shrimp. *Microb. Ecol*., **73**: 988-999. https://doi.org/10.1007/s00248-016-0910-x

Xu, C., Yagiz, Y., Hsu, W.Y., Simonne, A., Lu, J. and Marshall, M.R., 2014. Antioxidant, antibacterial, and antibiofilm properties of polyphenols from muscadine grape (*Vitis rotundifolia* Michx.) pomace against selected foodborne pathogens. *J. Agric. Fd. Chem*., **62**: 6640-6649. https://doi.org/10.1021/jf501073q

Zhang, Z., Yu, C., Wang, X., Yu, S. and Zhang, X.H., 2016. *Arcobacter pacificus* sp. nov., isolated from seawater of the South Pacific Gyre. *Int. J. Syst. Evol. Microbiol*., **66**: 542-547. https://doi.org/10.1099/ijsem.0.000751